Calibration Issues of the TFTR Multichannel Neutron Collimator.

S. von Goeler, L. C. Johnson,
M. Bitter, P. C. Efthimion, and A. L. Roquemore.

Princeton Plasma Physics Laboratory, Princeton NJ 08540.

Abstract: The calibration procedures for the detectors in the Neutron Collimator are reviewed. The absolute calibration was performed for the NE451 detectors, in situ, by moving a DT neutron generator in the TFTR vacuum vessel across each sight line. This calibration was transferred to other detectors in the same channel. Four new sight lines have been installed at a different toroidal location, which view the plasma through the vacuum vessel port cover rather than through thinned windows. The new detectors are cross-calibrated to the NE451 detectors with a "jog shot" procedure, where the plasma is quickly shifted in major radius over a distance of 30 cm. The jog shot procedure shows that scattered neutrons account approximately for 30% of the signal of the new central channels. The neutron source strength from the collimator agrees within 10 % with the source strength from global neutron monitors in the TFTR test cell. Detector non-linearity is discussed. Another special issue is the behavior of the detectors during T-puffs, where the DD/DT neutron ratio changes rapidly.

Presented at the 11th Topical APS Conference on High Temperature Plasma Diagnostics, Monterey CA, 12-16 May 1996.

I. INTRODUCTION.

The Multichannel Neutron Collimator[1,2,3,4] is an important diagnostic system on the Tokamak Fusion Test Reactor (TFTR), which measures radial profiles of the neutron emission from the hot plasma core and monitors the local fusion power density in the reactor. These measurements are highly relevant for future reactors, because the fusion power density in the core of TFTR during high power tritium shots[5] exceeds the fusion power density projected for the International Tokamak Experimental Reactor (ITER)[6].

The development of the TFTR Neutron Collimator has proceeded in several stages and was driven mostly by the extremely large dynamic-range requirements for deuterium-deuterium (DD) and deuterium-tritium (DT) operation of TFTR. The original neutron collimator[1] was equipped with NE451 detectors[7], which were absolutely calibrated in-situ, using a 14 MeV neutron generator inside the TFTR vacuum vessel.[8, 9] The NE451 system has provided most of the neutron profiles during the DD operation of TFTR.[2] However, the NE451 detectors, operating in the pulse counting mode, showed signs of saturation during high-power DD neutral beam injection and actually saturated during test tritium operation. Therefore, for DT operation less efficient detectors, the so-called ZnS Wafer Detectors,[3] were installed in the neutron collimator directly above the NE451 detectors. The ZnS Wafer Detector array was calibrated by transferring the calibration of the NE451 system, since both see the identical neutron flux. During very high power DT neutral beam injection, even the wafer system has exhibited signs of pulse-pile-up, and, therefore, the NE451 system was converted to current mode.[4] The calibration of the NE451 current mode system was again accomplished by transferring the calibration of the ZnS Wafer system during low power shots. In summer 1995, the neutron collimator diagnostic was extended further by drilling out two new sight lines through the basement floor of TFTR at Bay A[10], a location that is 180 degrees in toroidal direction apart from the Bay K NE451 system. The purpose of the extension was to obtain better spatial resolution in the plasma core. However, in an effort to suppress neutron statistical noise and to increase the temporal resolution, more efficient plastic detectors were used. Finally in February 1996, two additional sight lines were installed at Bay A, so that it contains now 4 channels. The new Bay A system is described at this conference by A. L. Roquemore,[11] and the layout of the collimator sight lines and details on the plastic detectors can be obtained from that paper.

The purpose of this paper is to report on the calibration and performance of the new Bay A channels. In Section II we discuss the "jog shot" calibration of the new channels. We found that the new detectors have a very large scattered neutron background, a result which is very important for the construction of the neutron collimator for ITER, because it shows that it is highly desirable to have a "see through" arrangement, where a detector views the plasma through thinned windows and has a viewing dump. During very high power DT operation, the Bay A plastic detectors showed a nonlinearity, which is discussed in Section III. In Section IV, we report an attempts to distinguish the DD and the DT scattered neutron background by evaluating a DD jog shot. In Section V we discuss the data evaluation during T gas puffing on TFTR.[12,13] The T puffs are important for analyzing particle transport. With this technique, we found a very large reduction of the tritium particle transport in the core of enhanced reversed shear (ERS) discharges on TFTR.

II. DT JOG SHOT CALIBRATION OF THE BAY A DETECTORS.

The jog shot procedure was invented by M. Zarnstorff[14] for the calibration of the motional Stark effect diagnostic (MSE). This technique was applied to the neutron collimator by L. C. Johnson[15] in order to fine-tune the calibration of the different radial collimator channels and to obtain high resolution profiles of the neutron emission. The calibration of the new Bay A detectors depends completely on the jog shot procedure, which has hence become an essential part of our operation. In a jog shot, a discharge is established with the plasma center at major radius R= 2.76 m. 500 ms after the start of NB injection the plasma is moved inward to a major radius R = 2.42 m in a time interval of 70 ms. By moving the plasma, the collimator effectively scans the radial neutron emission. Only moderate neutral beam heating (1 T beam and 2 D beams) is used, so that DT neutrons dominate (but do not saturate detectors). The jog time is chosen short enough, so that the plasma profile shape is conserved, and, on the other hand, sufficiently long so that the neutron traces are not degraded by statistical noise. In the jog shot evaluation procedure a normalized neutron signal from each channel is plotted versus the difference between the major radius of the sight line and the major radius of the plasma center (determined from magnetic measurements). More accurately, in order to accommodate the Shafranov shift and the conservation of toroidal magnetic flux, the ordinate y of Fig. 1 is chosen as

$$y \quad = \quad \int \varepsilon_n dl \quad \frac{S_{n1}}{S_n} \left(\frac{R_a + 0.3[\Delta - \Delta_1]}{R_{a1}} \right)^{-3/2}, \tag{1}$$

where $\int \varepsilon_n dl$ is the measured line integrated neutron emissivity in a particular channel, S_n is the neutron source strength, R_a the major radius of the last closed magnetic surface, and $\Delta = R_c - R_a$ is a quantity related to the Shafranov shift (R_c is the "center of gravity" of the radial plasma current density distribution, obtained from magnetic data). Magnetic diagnostics basically can not determine the exact position of the plasma center during the jog, however, it was found empirically that a suitable linear combination R_a and R_c makes the segments of the profile, each associated with a different channel, join together smoothly. The factor 0.3 provided the best results. The index 1 indicates that the quantity was taken at the beginning of the jog. The abscissa x is chosen as

$$x = \frac{R_{channel} - (R_a + 0.3[\Delta - \Delta_1])}{\sqrt{\frac{(R_a + 0.3[\Delta - \Delta_1])}{R_{a1}}}}, \tag{2}$$

where $R_{channel}$ is the major radius of the sight line of a collimator channel.

Jog profiles y(x) of eight Bay K and four Bay A neutron collimator channels are shown in Fig. 1, where subfigure (a) shows profiles obtained before the calibration of the Bay A channels and (b) after the calibration. The thin curves represent the Bay K channels. They reflect the original calibration of the collimator with the in situ DT neutron generator, and only minor adjustments to the calibration factors and background correction were made to merge all eight curves into one smoothly fitting ensemble. The thick curves represent the new Bay A channels. In the calibration process three constants are adjusted so that the Bay A signals fall as close as possible on top of the Bay K jog profile, as shown in subfigure (b). The three constants are (1) the major radius of the intersection of the sight line with the horizontal mid plane, (2) the calibration factor for the signal amplitude, and (3) the scattered neutron background correction factor. It is obvious that the calibration procedure gives quite accurate results for the central channels that view the maximum of the emission profile and leaves more ambiguity for the outer channels.

We have also plotted in Fig. 1b the scattered neutron background correction, that was used in the evaluation of the data. The scattered neutron signal was multiplied by the same normalization factor that was used to obtain the jog profile y from the line integrated neutron emissivity. For the eight Bay K channels, the scattered neutron correction is very small (i. e. 2% to 3% of the signal for the central channels). For the new Bay A channels, however, the scattered neutron correction represents 25 to 45% of the central intensity. This is the very important result for the construction of future collimators of fusion reactors, mentioned in the introduction. The Bay K collimator is a "see through" collimator, where a detector views the plasma through thinned 3 mm thick stainless steel windows. Also the port cover on top of the vacuum vessel has been thinned and the space in-between toroidal field coils serves as a viewing dump. At Bay A, in contrast, the sight lines go right through the 30 mm thick port covers of the vacuum vessel, and we consequently expect to encounter a roughly ten times larger scattered neutron and gamma background. It will become impossible to measure the neutron intensity in the outer channels at Bay A, where the background is much larger than the signal, unless detectors can be found that discriminate efficiently between the original 14 MeV DT neutrons and the scattered neutrons (which, e.g. for elastic scattering with iron, have nearly the same energy).

III. DETECTOR NON-LINEARITY.

During DT operation, the neutron energy flux increases by more than a factor of 100 (i. e. the detector system has to have an extremely large dynamic range). The change from DD to DT injection is accommodated in the Bay K system by reducing the high voltage on the photomultipliers for DT discharges. With the more efficient plastic scintillators of the new Bay A system, the photomultipliers (PMT) required less gain, and we reduced the number of dynodes of the PMT. However, because of the reduction, the voltage per stage during high power DT discharges became so low, that the PMTs showed signs of non-linearity. This was measured by mounting a photo diode, usually a large area surface barrier detector, besides the PMT on the plastic scintillator. The ratio of the PMT to the diode signal during one high power DT shot is plotted versus the PMT signal in Fig. 2a. The data are fitted by a parabola (the thin line in Fig. 2a), which provides two correction constants for our computer analysis program. Fig. 2b and 2c show PMT signals with and without correction and, for comparison, the photo diode signal (dotted). This evaluation procedure provided satisfactory results up to the highest injection powers. To demonstrate the performance of the system, we plot the ratio of the neutron source strengths from the collimator and from a global neutron monitor, the U235 fission chamber NE-CU-S3 in the TFTR test cell, versus the source strength of the fission chamber in Fig. 3. It is apparent that the two measurements agree within 5%. The somewhat larger discrepancies for very small neutron fluxes are partially due to the presence of DD neutrons and partially due to the fact that the U235 fission chamber CU-S3 does not provide satisfactory results for source strengths smaller than 1×10^{17} n / sec.

Although the source strength ratio in Fig. 3 was obtained for the whole system, consisting of 8 Bay K channels and only 2 Bay A channels, these data also reflect on the performance of the Bay A detectors, because the two Bay A channels view the plasma core and are on a par with the two central Bay K channels in the determination of the neutron source strength. Lastly, we originally had hoped that the photodiode output would become the neutron signal for DT operation. However, it exhibits an extremely large shot noise that is due, probably, to a few direct neutron interactions with the surface barrier detector.

IV. DD JOG SHOT FOR THE SCATTERED DD NEUTRON BACKGROUND.

During tritium beam injection, the 14 MeV DT neutrons dominate the neutron production, and the contribution of the 2.5 MeV DD neutrons can be neglected. During DD operation, on the other hand, the plasma usually contains a small amount of tritium which is left over from previous DT operation, and, therefore, the number of DD and DT neutrons is typically of comparable size. The problem is then, how to evaluate DD discharges. In this section, we try to evaluate a DD jog shot in order to obtain the scattered neutron background correction for DD neutrons. The result will be that the background correction for DD neutrons, relative to the neutron signal produced by DD neutrons, is of very similar size as that for DT neutrons.

First we assume for simplicity that the DD over DT neutron ratio does not depend on plasma radius. Hence we can obtain the DD/DT neutron ratio from global neutron detectors.[16] For the NE451 system at Bay K, which has a very small scattered background component, the sensitivity of the detector signals I_ν in channel ν towards DT and DD neutrons is known and can be described by the equation

$$I_\nu \;=\; \int \varepsilon_{n_{DT}} dl_\nu + 0.3 \int \varepsilon_{n_{DD}} dl_\nu . \qquad (3)$$

The same relationship holds then for the neutron source strength from the collimator,

$$S_{n-coll} \;=\; \sum_{\nu} I_{\nu} \Delta R_{\nu} \;=\; S_{n_{DT}} + 0.3\, S_{n_{DD}}, \tag{4}$$

where ΔR_{ν} is the distance between sight lines in the horizontal midplane. On the other hand, the U235 fission detector NE-CU-S2 in current mode has a different dependence on the DD and DT source strength

$$S_{n-CUS2} \;=\; 1.29\, S_{n_{DT}} + S_{n_{DD}}. \tag{5}$$

Therefore, the number of DT and DD neutrons can be determined from the measured source strengths $S_{n\text{-}CUS2}$ and $S_{n\text{-}coll}$. Provided the DT / DD ratio does not depend on plasma radius, the DT as well as the DD neutron emissivity can be determined.

The results from a DD jog shot are shown in Fig. 4, where the "jog profiles" of the DD neutron emission are plotted in the usual fashion as outlined in Sect. 2. Before we discuss this figure, we want to mention a small inconsistency in our analysis. During the DD jog, the measured DD/DT ratio exhibits a short dip, which causes a significant distortion of the DT as well as the DD profile. Although there exist the possibility that fast DD and DT ions are accelerated during the jog, the dip seemed to us unphysical, because we would expect that fast ion acceleration would create a hump rather than a dip in the DD concentration. Consequently we have smoothed out the dip, although we do not have a good rational for it. Due to increased statistical noise during DD operation, the data in Fig. 4 are not as smooth as the DT data in Fig. 1. The ratio of background to neutron signal for the DD neutrons is very similar to the one obtained for DT neutrons (Fig. 1). Therefore, the detector signal Y_{ν} of the Bay A detectors before background subtraction can very approximately be described by the equation

$$Y_{\nu} \;=\; a_{\nu}\left(I_{\nu_{DT}} + 0.3 I_{\nu_{DD}}\right) + b_{\nu}(R_{pl}, R_{\nu})\left[S_{DT} + 0.3 S_{DD}\right], \tag{6}$$

where the a_{ν} and b_{ν} are the calibration factor and the background correction factor obtained from the tritium jog shot. The result that the NE102A and the NE451 have the same DD/DT sensitivity ratio and also the same DD/DT background sensitivity ratio is somewhat surprising, it can not be strictly correct and can only be coincidental. Both detectors were designed for a high DT neutron efficiency (the NE 451 detector by design, the plastic detectors because of the six inch length), and they accidentally turn out to have a similar small relative efficiency of 0.3 for low energy neutrons. The DD background correction, is not very accurate, because (a) the statistics during the relatively short duration of the jog are not very favorable, and (b) the DD signal and the DD correction was smaller than the DT signal and the DT correction (although there were more DD neutrons emitted than DT neutrons). Radiation transport computations indicate that the ratio of energy fluxes of gamma rays to DD neutrons is much larger than the γ-to neutron energy flux ratio for DT neutrons.[17] Therefore, the DD jog results indicate that the background is probably caused by scattered neutrons, and not by scattered gamma rays. A more satisfactory solution to this problem will hopefully be obtained when the contributions from DT neutrons, DD neutrons, and gamma rays are measured separately.[18]

V. EVALUATION PROCEDURES DURING TRITIUM PUFFS

During the past year, the Enhanced Reversed Shear (ERS) mode of tokamak operation[19] has been subject of intense investigation on both the TFTR tokamak in Princeton and the DIII-D tokamak in San Diego. One of the important observations is the very long ion particle confinement time[20] obtained with a tritium gas puffing technique,[21,22] where a trace amount of tritium is released by a fast gas valve near the plasma edge. The inward and outward transport of tritium is observed by monitoring the 14 MeV neutron emission with the neutron collimator. These experiments involve a number of difficult calibration issues, which we want to discuss in this section.

The basic experimental difficulty with the tritium gas puff experiments is that the neutrons are predominantly DD neutrons before the puff, whereas DT neutrons dominate shortly afterwards (Fig. 5c). The basic technique used to evaluate these shot is to subtract two identical shots, one with a T-puff, the other one without T-puff. It is usually difficult to find completely identical shots, for instance for shot #88171 (the subtraction shot in Fig. 5), there occurred a few neutral beam faults. Therefore, we slightly "adjust" the subtraction shot so that its neutron source strength closely matches the neutron source strength of the main shot directly before the T-puff . For example in Fig. 5d, the neutron source strength from the fission detector NE-CU-T2 and all collimator signals of the subtraction shot #88171 are multiplied with an adjustment factor of 1.09 and offset by -2.8% in order obtain the same absolute value and the slope of the source strength before the puff as in shot #88170. Presuming that the small tritium release at the plasma edge does not change the deuterium recycling, we assume then that the difference signal is due solely to DT neutrons, for which we have reliable calibration and background subtraction factors. In Fig. 5e, we show the subtracted signals for the U235 fission detector NE-CU-T2 and the Neutron Collimator for shots #88170 and #88171. The development of the non-inverted subtracted radial profiles is shown in Fig. 6a, which consists of Bay K data with NE451 detectors only. In contrast, Fig. 6b also includes two high efficiency plastic detectors from Bay A. The profiles in subfigure (b) have humps at radii R=2.59 m and R = 2.82 m, which correspond to the location of the plastic detectors. The humps are not there before the T-puff and they slowly disappear after the T puff. The occurrence of these humps shows that the plastic and the NE451 detectors exhibit a different temporal behavior; the plastic detectors rise at a faster rate than the Ne451 detectors early during the T puff. This discrepancy has not yet been fully resolved. It is believed to be due to the different size of background subtraction for the two detectors, although other possible effects can not be excluded. For instance, early during the puff, before the tritium penetrates to the center, the neutrons are emitted from a shell, which produces an increased background for the central channels. However, this effect was modeled and seems too small to explain the discrepancy. As far as the interpretation of the T-puff experiments is concerned, there remain two issues: (1) Considerable uncertainty exists for the peak intensity, because there are no data directly in the peak region from Bay K data only. (2) Although we are convinced that also the Bay A detectors would show the same hollow profiles and the consecutive strong peaking as the Bay K detectors, there is a discrepancy between the detectors that indicates an unknown systematic error. The Abel inverted Bay K data by themselves (Fig. 6c) exhibit beautiful hollow profiles during the early stages of the T-puff, which fill in after 80 msec and then become very peaked with the peak intensity still increasing 230 msec after the T-puff, until at 2.9 sec the high power neutral beam injection is turned off.

Acknowledgments: We are indebted to M. Bell for providing the magnetic wave forms for the jog shot evaluation. T. Holoman and J. Gorman have provided much needed technical assistance. J. Montague and M. Diesso helped with the computer hardware and software. The support of D. Johnson and K. McGuire is gratefully acknowledged. This work was supported by US. DoE. Contract DE-AC02-76CH03073.

[1] A. L. Roquemore, R. C. Chouinard, M. Diesso, R. Palladino, J. D. Strachan, and G. Tait: Rev. Sci. Instrum. **61**, 3163 (1990).

[2] L. C. Johnson: Rev. Sci. Instrum **63**, 4517 (1992).

[3] A. L. Roquemore, L.C. Johnson, and S. von Goeler: Rev. Sci. Instrum. **66**, 916 (1995).

[4] S. von Goeler, et al.: Rev. Sci. Instrum. 67, p 473 (1996).

[5] R. J. Hawryluck, H. Adler, P. Alling, C. Ancher, H. Anderson, et al.: Proc. of the 15th Intern. Conf. on Plasma Physics and Nuclear Fusion Research, Seville (Spain) (International Atomic Energy Agency, Viennna) , Vol. 1, p. 11 (1995).

[6] A. E. Costley: Rev. Sci. Instrum. **66**, p. 297 (1995).

[7] Manufactured by NUCLEAR ENTERPRISES Inc., San Carlos CA 94070.

[8] J. D. Strachan, .C. W. Barnes, M. Diesso, D. Jasby, L. C.Johnson et al.: Rev. Sci. Instrum. **66**, p. 897, (1995).

[9] D. Jassby, C. W Barnes, L. C. Johnson, A. L. Roquemore, J. D. Strachan, et al.: Rev. Sci. Instrum. **66**, p. 891 (1996).

[10] A. L. Roquemore, et al: "Upgrade to the Multichannel Neutron Collimator", Proc. IEEE Meeting on Fusion Engineering, Champaign Illinois, (1995).

[11] A. L. Roquemore, M. Bitter, L. C. Johnson, and S. von Goeler: "Recent Expansion of the TFTR Multichannel Neutron Collimator", proceedings of this conference.

[12] L. C. Johnson, P. C. Efthimion, J. D. Strachan, E. J. Synakowski, M. Zarnstorff et al.: 21st EPS Conf.(Montpellier), Europhysics Conf. Abstracts **18B**, Part 1, p.182 (1994).

[13] P. C. Efthimion, L. C. Johnson, J. D. Strachan, E. J. Synakowski, M. Zarnstorff, et al.: Phys. Rev. Lett. **75**, p.85 (1995).

[14] M. Zarnstorff, S. Batha, A. Janos, F. Levinton, and the TFTR Group, Proc. Workshop on Local Transport Studies in Fusion Plasmas, Varenna, (J. Callen, G. Gorini, and Sindoni Eds.) SIF, Bologna, p. 257 (1993), and F. M. Levinton, S. H. Batha, M. Yamada, and M. Zarnstorff: Phys. Fluids B **5**, p. 2554 (1993).

[15] L. C. Johnson, Cris Barnes, R. E. Bell, M. Bitter, R. Budny, et al.: "Fusion Product Measurements in DT Plasmas in TFTR", in Proc. International Workshop on ITER Diagnostics, Varenna, Italy (1995).

[16] D. L. Jassby, H. Hendel, and H.-S. Bosch, Rev. Sci. Instrum **59**, p. 1688 (1988), and E. Ruskov, W. Heidbrink, H. Duong, A. L. Roquemore, and J. Strachan: Rev. Sci. Instrum. **66**, p. 919 (1995).

[17] Long Po Ku, private communication.

[18] M. Bitter, L. C. Johnson, L.-P. Ku, A. L. Roquemore, and S. von Goeler: "Distinction between DD and DT neutrons", proceedings of this conference.

[19] F. M. Levinton, M. Zarnstorff, S. Batha, M. Bell, R. Bell, et al.: Phys. Rev. Lett. **75**, p. 4417 (1995).

[20] P. Efthimion et al, APS Bulletin **40**, p. 1870 (1996), and S. von Goeler et al, APS Bulletin **40**, p. 1768 (1996) unpublished.

[21] L. C. Johnson, :P. C. Efthimion, J. D. Strachan, E. J. Synakowski, M. Zarnstorff et al.: 21st EPS Conf. (Montpellier), Europhysics Conf. Abstracts **18B**, Part 1, p.182 (1994).

[22] P. C. Efthimion, L. C. Johnson, J. D. Strachan, E. J. Synakowski, M. Zarnstorff, et al. Phys. Rev. Lett. 75, p.85 (1995).

Figure Captions:

Fig. 1: DT jog shot calibration of four Bay A detectors. Plotted is a normalized chord-integrated neutron emissivity divided by the neutron source strength versus the difference between collimator-channel radius and the plasma major radius. The exact form of the normalization factors is discussed in the text. Subfigure (a) shows the data before calibration. The heavy curves represent the Bay A channels, the thin curves the Bay K channels. The numbers indicate channel numbers (at the start of the jog above the curve, at the end of the jog below the curve). Subfigure (b) shows jog profiles after calibration. Plotted is also the scattered background correction signal during the jog, which has been multiplied with the same normalization factors.

Fig. 2: Nonlinear detector response for high power tritium operation. The scintillation light emission of the 10.8 $\times$ 3.8 $\times$ 12.7 cm plastic NE102A detector is measured independently by a photo multiplier tube (PMT) and by a photo diode. In subfigure (b) the signals from the diode (dotted) and from the PMT (solid) are plotted vs. time. The PMT signal is normalized, so that the area underneath both curves is equal. In subfigure (a) the same data are used to plot the ratio of the two signal vs. the PMT signal. The thin line represents a parabolic fit, which yields two correction parameters. The correction parameters are averaged over many shots. In subfigure (c) the corrected PMT signal is compared with the diode signal. The two are now practically indistinguishable, except that the diode signal has more noise.

Fig. 3: The ratio of the neutron source strength S_{coll} from the collimator in current mode over the source strength $S_{NE\text{-}CU\text{-}S3}$ from a U235 fission chamber in current mode versus the source strength of the fission detector. The figure illustrates that the collimator (with the nonlinear correction for the Bay A channels) provides accurate results even in the most powerful DT discharges.

Fig. 4: Jog profiles in a DD discharge for the determination of the DD neutron scattering background. (Same type of plot as Fig. 1b, two Bay-A channels only).

Fig. 5: Evaluation procedure for tritium gas puffs. From the traces of shot #88170, which had a tritium puff at time 2.67 sec, we subtract the corresponding traces of the nearly identical shot #88171, which had no T-puff. Both discharges had an ERS transition approximately at time 2.6 sec. The neutron source strengths after subtraction derived (1) from the collimator and (2) from the U235 fission chamber NE-CU-T2 are nearly identical and are believed to consist only of the DT neutrons from the trace tritium of the puff.

Fig. 6: Subtracted radial profiles of the neutron emission during tritium gas puffing. Subfigure (a) shows non inverted profiles from the Bay K system with NE 451 detectors only. Subfigure (b) shows the same data including two Bay A plastic detectors at R = 259 cm and at R = 282 cm. Subfigure (c) shows Abel-inverted profiles (Bay K only), that exhibit hollow neutron emission profiles directly after the tritium puff. The hollow profiles fill in approximately 60 msec after the puff and then become peaked. The peaking and strong increase of the neutron emission continues for 230 milliseconds until the high power beam injection is shut off.

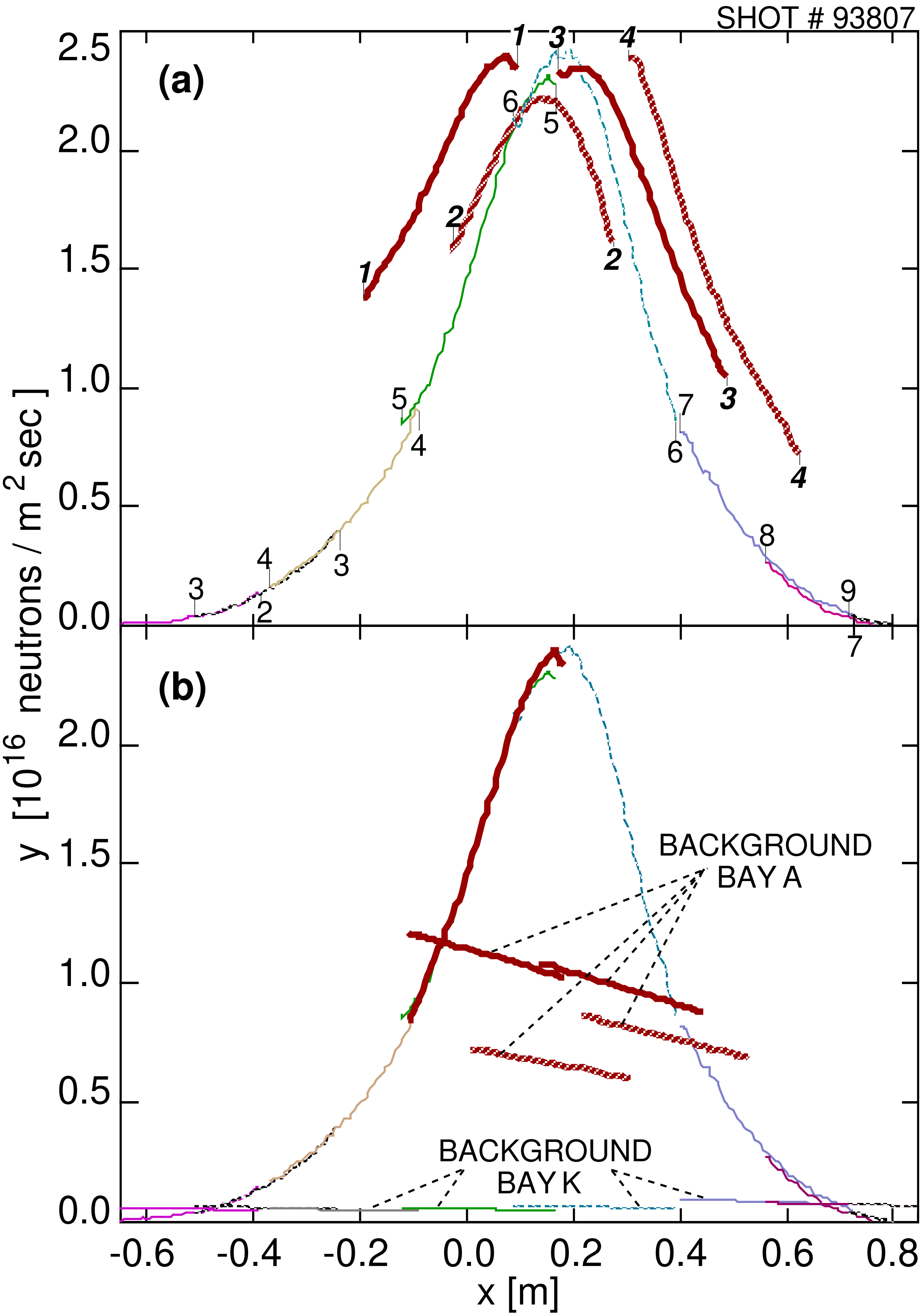
SHOT # 93807
(a)
(b)
BACKGROUND
BAY A
BACKGROUND
BAY K
y [10^{16} neutrons / m^{2}sec]
x [m]
-0.6
-0.4
-0.2
0.0
0.2
0.4
0.6
0.8
0.0
0.5
1.0
1.5
2.0
2.5

Figure 1

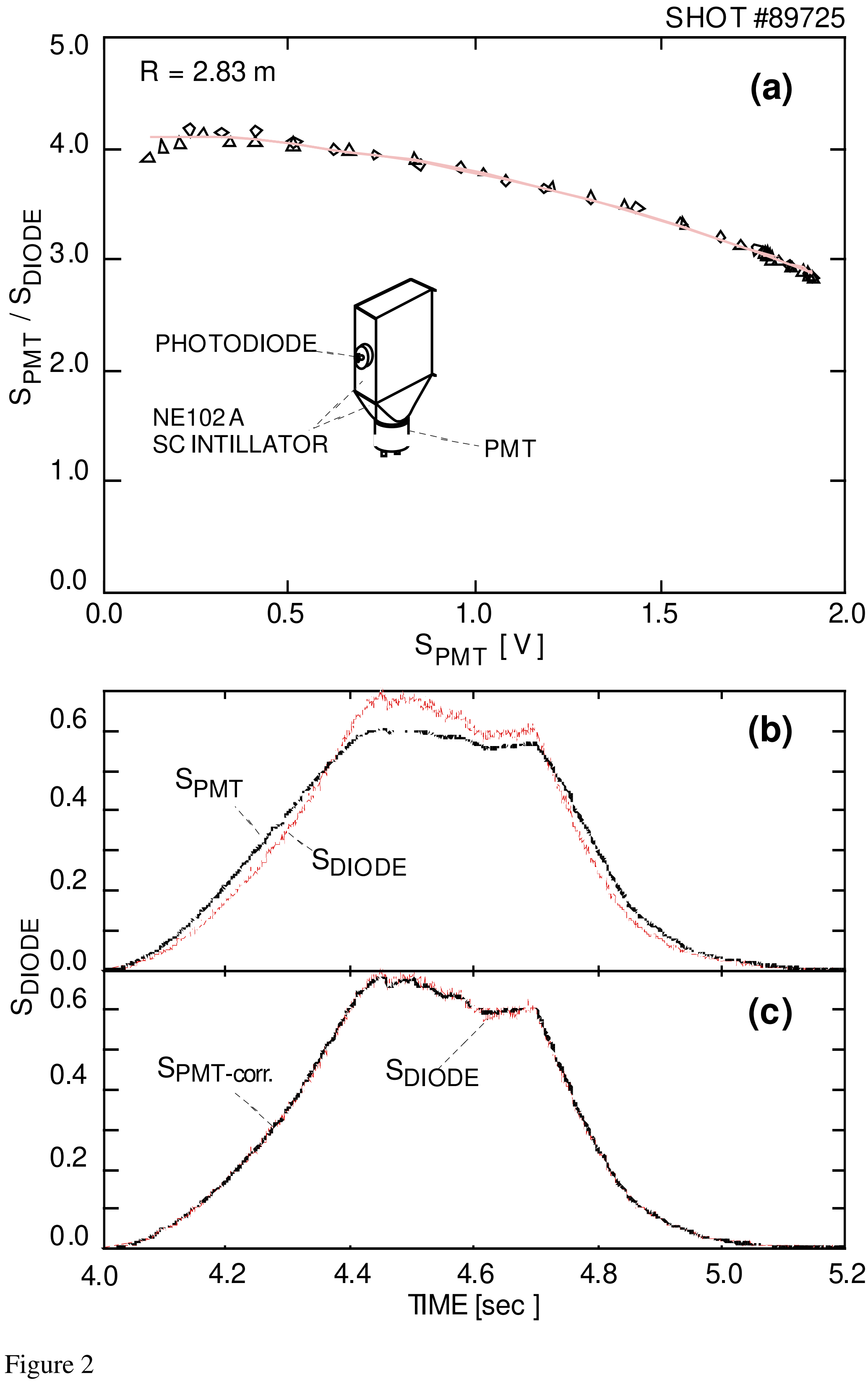

SHOT #89725
R = 2.83 m
(a)
PHOTODIODE
NE102 A
SC INTILLATOR
PMT
S_{PMT} / S_{DIODE}
S_{PMT} [V]
(b)
S_{PMT}
S_{DIODE}
(c)
$S_{PMT\text{-}corr.}$
S_{DIODE}
S_{DIODE}
TIME [sec]

Figure 2

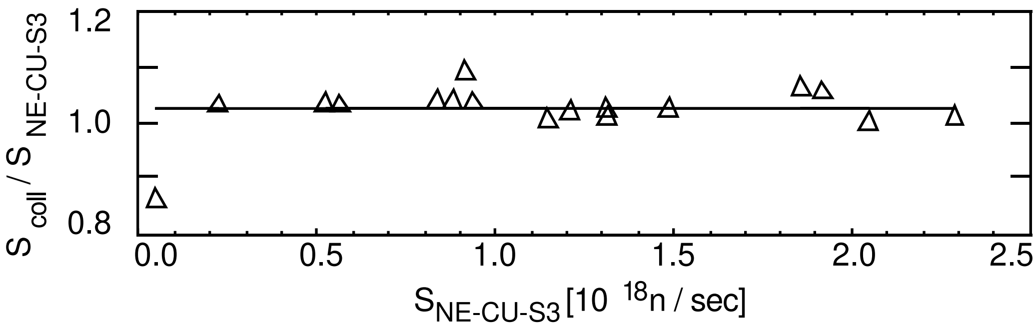
1.2
1.0
0.8
$S_{coll} / S_{NE\text{-}CU\text{-}S3}$
0.0
0.5
1.0
1.5
2.0
2.5
$S_{NE\text{-}CU\text{-}S3}$ [10^{18} n / sec]

Figure 3

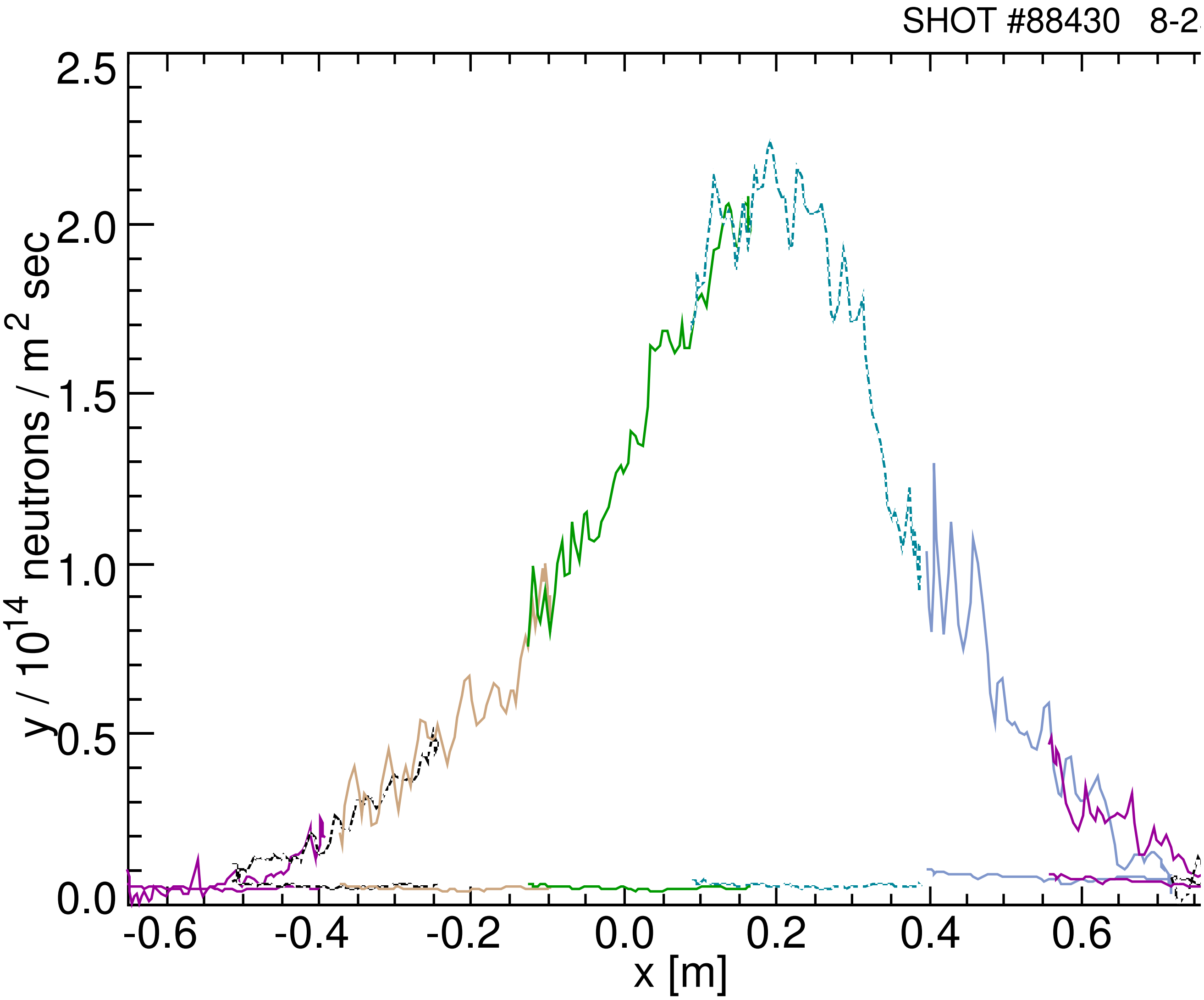
SHOT #88430 8-2
2.5
2.0
1.5
1.0
0.5
0.0
y / 10^{14} neutrons / m^2 sec
-0.6
-0.4
-0.2
0.0
0.2
0.4
0.6
x [m]

Figure 4

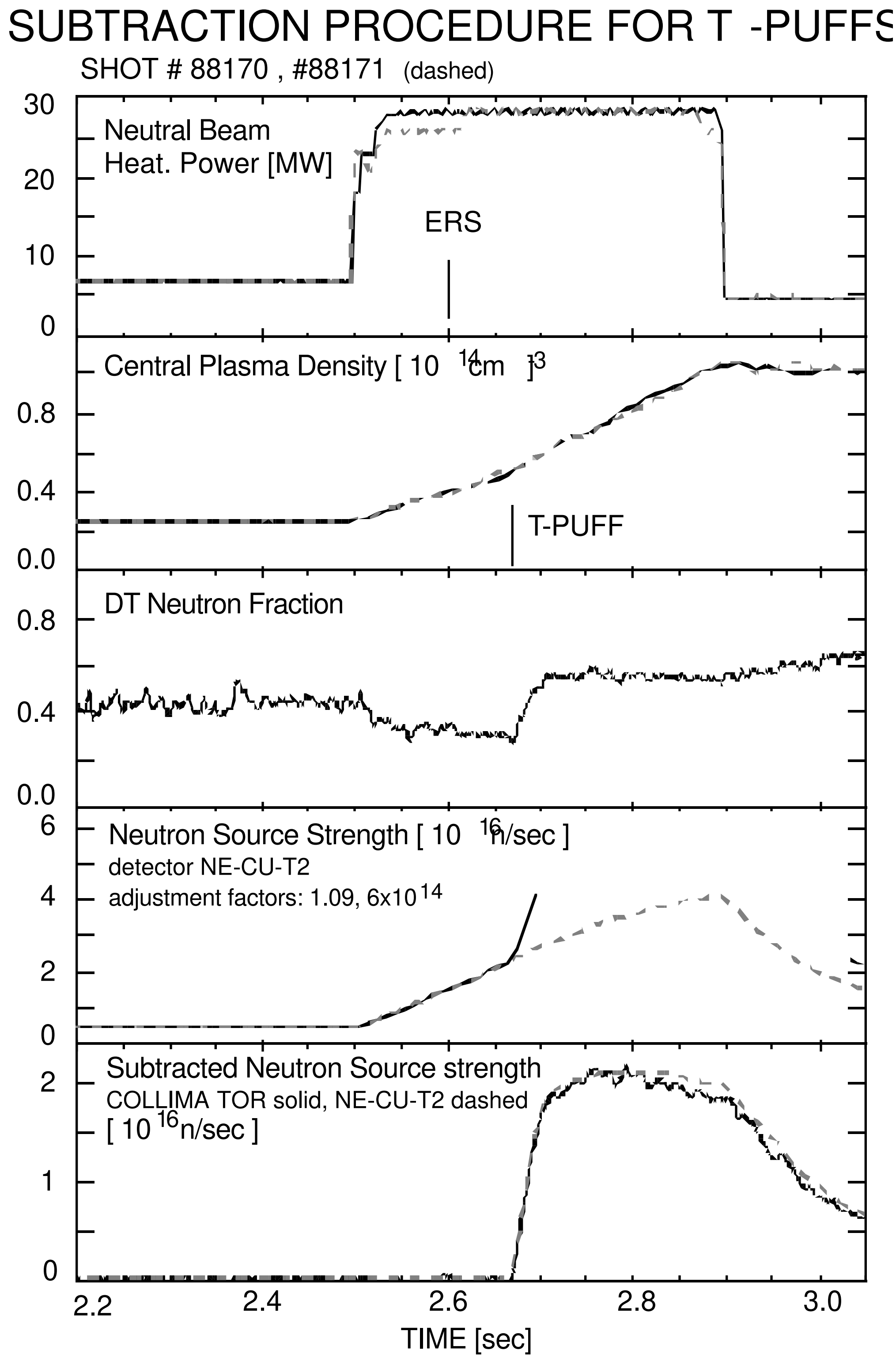

SUBTRACTION PROCEDURE FOR T -PUFFS
SHOT # 88170 , #88171 (dashed)
Neutral Beam
Heat. Power [MW]
ERS
Central Plasma Density [10 14 cm -3]
T-PUFF
DT Neutron Fraction
Neutron Source Strength [10 16 n/sec]
detector NE-CU-T2
adjustment factors: 1.09, 6x10 14
Subtracted Neutron Source strength
COLLIMA TOR solid, NE-CU-T2 dashed
[10 16 n/sec]
TIME [sec]

Figure 5

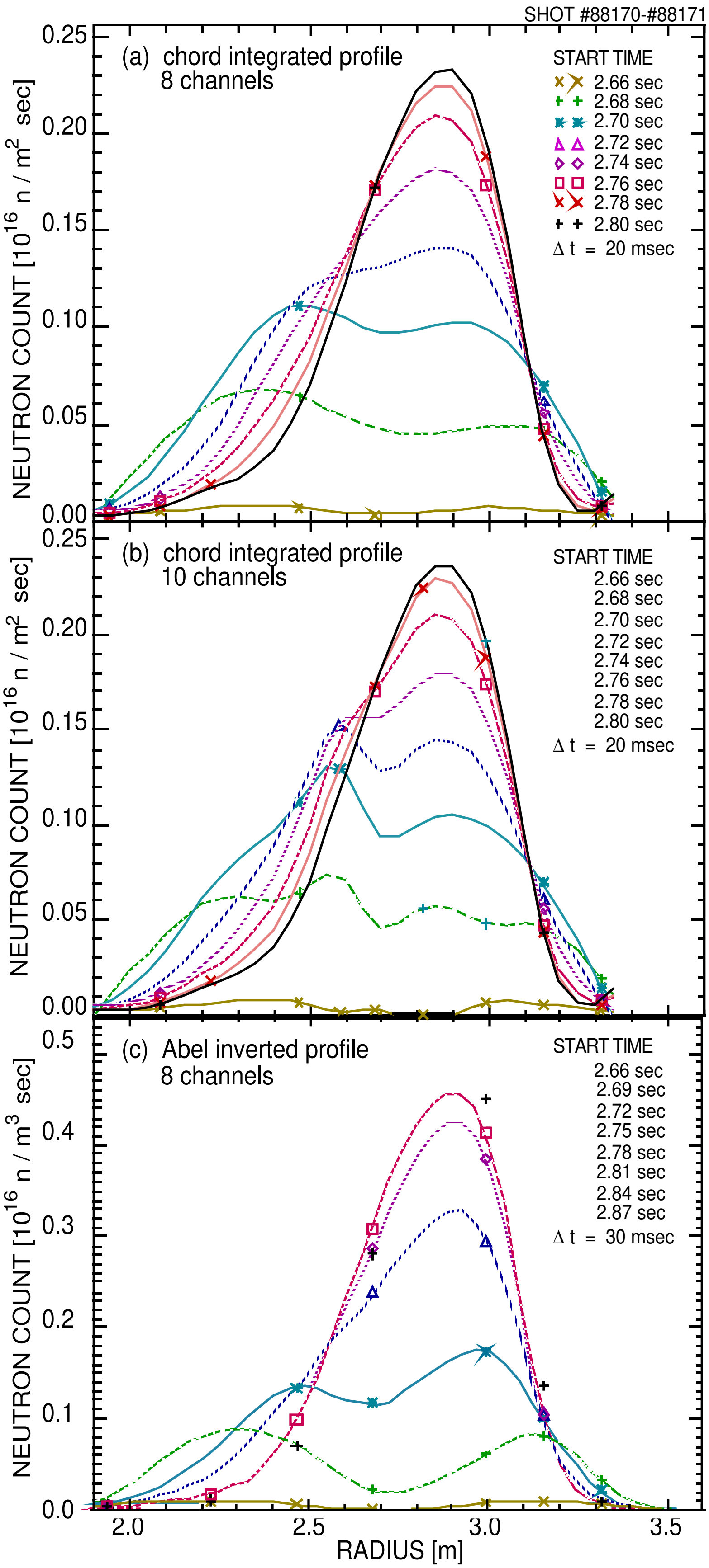
SHOT #88170-#88171
(a) chord integrated profile
8 channels
START TIME
2.66 sec
2.68 sec
2.70 sec
2.72 sec
2.74 sec
2.76 sec
2.78 sec
2.80 sec
Δ t = 20 msec
(b) chord integrated profile
10 channels
START TIME
2.66 sec
2.68 sec
2.70 sec
2.72 sec
2.74 sec
2.76 sec
2.78 sec
2.80 sec
Δ t = 20 msec
(c) Abel inverted profile
8 channels
START TIME
2.66 sec
2.69 sec
2.72 sec
2.75 sec
2.78 sec
2.81 sec
2.84 sec
2.87 sec
Δ t = 30 msec
NEUTRON COUNT [10^16 n / m^2 sec]
NEUTRON COUNT [10^16 n / m^3 sec]
RADIUS [m]

Figure 6